Izvestiya, Atmospheric and Oceanic Physics

Vol. 24, No. 9, 1988
UDC 551.513

A Low-Order Model of the Effect of Orography on Large-Scale Atmospheric Flows

I. A. PISNICHENKO

Institute of Atmospheric Physics, USSR Academy of Sciences

An eight-component barotrophic model describing large-scale atmospheric currents above an orographically nonuniform spherical earth is constructed. The dependence of steady-state modes of the model on the magnitude and structure of the orographic function is studied. For some values of the characteristics of the orographic function and the external drive, the stream line pattern obtained for steady-state solutions representing small values of the circulation index has the form typical of split blocking.

Specialists in dynamic meteorology still are not in agreement regarding the roles of the various mechanisms that generate and maintain blocking situations. Rather numerous models of the phenomenon have been offered, but none of them is exhaustive. The mean reason is apparently that the term "blocking structure" embraces large-scale atmospheric structures of highly varied types [1]. According to Obukhov et al. [1], three principal types of blocking structures are now distinguished: meridional blocking, split blocking, and omega blocking. The geographic position, type of evolution and frequency of occurrence of blocking situations are highly dependent on the time of year. The models proposed to explain these situations fall into two main classes. Some assign the main role to external factors such as orography and nonuniform heating of the atmosphere from below as a result of the presence of the continents and oceans [2-5]. Models of this type are usually linear or quasilinear. They have been most successful in the study of meridional blocking [3]. The other class consists of models that treat nonlinear interactions (Rossby waves, singular geostrophic eddies) as the principal mechanism giving rise to blocking structures [6-8]. These models are rather effective in reproducing the flow patterns in split blocking, but they do not explain the geographic distribution of blocking situations.

Low-order spectral models are widely used in the structure of blocking [9, 10]; they can be used to investigate in pure form the roles played by the various structures in blocking, allowing a better understanding of the phenomenon.

The simplest model of this type is the triplet, which has been used by Paegle [11] and the present author [12] to study the effect of orography on the interaction of Rossby waves with a zontal flow of the solid-rotation type. Despite its crudeness, this model can be used for the qualitative study of certain characteristics of meridional blocking. In any investigation, even qualitative, of split blocking, which has a more complex meridional structure, more complex spectral models must be used [4, 10]. An attempt to apply a rather simple low-order model to the analysis of split blocking has been made by Källen [10], who used a six-component barotropic model on a sphere in which the orography was described by single spherical harmonic $\xi = C_n^m P_n^m(\theta)\sin m\varphi$, and in which the solution sought for the stream function contained two components modeling the zonal flow, $\tilde{\psi} = (-\alpha(t)\cdot P_1^0(\theta) + \beta(t) P_3^0(\theta))\,\omega a^2$ and four components representing the nonzonal flow, $\hat{\psi} = (A_n^m(t)\sin m\varphi + B_n^m(t)\cos m\varphi) P_n^m(\theta) + (A_{n+2}^m(t)\sin m\varphi + B_{n+2}^m(t)\cos m\varphi) P_{n+2}^m(\theta)$. This is the simplest nontrivial generalization of the triplet to the case of interaction of Rossby waves with a zonal flow different from solid rotation with allowance for orography. Källen studied steady-state solutions of the model, their energetics and their dependence on certain parameters (the value of the orographic function and the magnitude of the phase angle between the orography function and the nonzonal forcing function). But the model could not reproduce the flow pattern responsible for split blocking.

We believe that when analyzing blocks it is more natural to use an eight-component model, derived from that described above by adding two more modes in the nonzonal component of the flow, $(A_{n-2}^m(t)\sin m\varphi + B_{n-2}^m(t)\cos m\varphi) P_{n-2}^m(\theta)$: as a result of interaction of zonal component ψ_3^0 with the mode ψ_n^m, the modes ψ_{n+2}^m and ψ_{n-2}^m are generated and the flows of enstrophy and energy to these modes as a result the interaction are roughly of the same mag

We begin with the equation for the evo of the quasigeostrophic potential vorticity w allowance for orgraphic nonuniformities on a spherical earth, based on the barotropic model of the atmosphere:

$$\frac{\partial \Delta\psi}{\partial t} + (\psi, \Delta\psi + l + \xi) = \hat{\varepsilon}(\Delta\psi_0 - \Delta\psi), \qquad (1)$$

where ψ is the stream function, $l = 2\pi\cos\theta$ is the Coriolis parameter, l_{avg} is the mean value of

0001-4338/90/2409-0004$18.00/1

the Coriolis parameter, $\xi = l \operatorname{avg} \hat{h}/H_0$ is the orographic function, H_0 is the height of the uniform atmosphere, $\hat{h}$ is the deviation of the relief from the mean level, $\hat{\varepsilon}$ is the coefficient of relaxation resulting from Ekman friction, ψ_0 is the forcing function, which models external sources of vorticity, a is the radius of the earth, and ω is the angular velocity of the earth,

$$(a, b) = \frac{1}{a^2 \sin\theta}\left(\frac{\partial a}{\partial \theta}\frac{\partial b}{\partial \lambda} - \frac{\partial a}{\partial \lambda}\frac{\partial b}{\partial \theta}\right).$$

We distinguish the zonal component of the flow and deviations from zonality. Neglecting the effect of interaction between nonzonal components, we obtain the following system of equations (where tilde denotes zonally averaged quantities and the prime the deviations from zonally averaged values):

$$\frac{\partial \Delta\tilde{\psi}}{\partial t} - \frac{1}{a^2 \sin\theta}\frac{\partial}{\partial \theta}\left[\widetilde{\frac{\partial \psi'}{\partial \lambda}\xi}\right] = \hat{\varepsilon}(\Delta\tilde{\psi}_0 - \Delta\tilde{\psi}),$$

$$\frac{\partial \Delta\psi'}{\partial t} + \frac{1}{a^2 \sin\theta}\left[\frac{\partial \tilde{\psi}}{\partial \theta}\frac{\partial}{\partial \lambda}(\Delta\psi' + \xi) - \frac{\partial \psi'}{\partial \lambda}\frac{\partial}{\partial \theta}(\Delta\tilde{\psi} + l)\right] = \hat{\varepsilon}(\Delta\psi_0' - \Delta\psi'). \quad (2)$$

Describing the orography with a single spherical harmonic $\xi = C_n^m P_n^m(\theta)\cdot \sin m\lambda$ and choosing as a finite-dimensional approximation of the system solution the modes just noted, we arrive at a system of eight ordinary differential equations which in dimensionless form are

$$\frac{d\alpha}{d\tau} = -d_3 b_n C + \varepsilon(\alpha_0 - \alpha),\quad \frac{d\beta}{d\tau} = -d_4 b_n C + \frac{35}{12}d_3 C(b_{n+2} + b_{n-2}) - \frac{35}{6}d_3(2n-1)(a_n b_{n-2} - a_{n-2}b_n) - \frac{35}{6}d_3(2n+3)(a_{n+2}b_n - a_n b_{n+2}) + \varepsilon(\beta_0 - \beta),$$

$$\frac{da_{n-2}}{d\tau} = \left(d_{10}\alpha + d_{11}\beta - \frac{2m}{(n-2)(n-1)}\right)b_{n-2} - d_{12}\beta b_n - \varepsilon a_{n-2},\quad \frac{db_{n-2}}{d\tau} = -\left(d_{10}\alpha + d_{11}\beta - \frac{2m}{(n-2)(n-1)}\right)a_{n-2} + d_{12}\beta a_n - d_{15}\beta C - \varepsilon b_{n-2},$$

$$\frac{da_n}{d\tau} = \left(d_1\alpha + d_2\beta - \frac{2m}{n(n+1)}\right)b_n - \beta(d_5 b_{n-2} + d_6 b_{n+2}) + \varepsilon(a_{n0} - a_n),\quad \frac{db_n}{d\tau} = -\left(d_1\alpha + d_2\beta - \frac{2m}{n(n+1)}\right)a_n + \beta(d_5 a_{n-2} + d_6 a_{n+2}) + \frac{m\alpha C}{n(n+1)} + d_{13}\beta C + \varepsilon(b_{n0} - b_n),$$

$$\frac{da_{n+2}}{d\tau} = \left(d_7\alpha + d_8\beta - \frac{2m}{(n+2)(n+3)}\right)b_{n+2} - d_9\beta b_n - \varepsilon a_{n+2},\quad \frac{db_{n+2}}{d\tau} = -\left(d_7\alpha + d_8\beta - \frac{2m}{(n+2)(n+3)}\right)a_{n+2} + d_9\beta a_n - d_{14}\beta C - \varepsilon b_{n+2}. \quad (3)$$

Here, $\tau = t\omega$, $C = C_n^m/\omega$, $\varepsilon = \hat{\varepsilon}/\omega$, $(a_n b_n) = (A_n^m, B_n^m)/\omega a^2$, $(a_{n-2}, b_{n-2}) = (A_{n-2}^m, B_{n-2}^m)(n-m)(n-m-1)/[\omega a^2(2n-3)(2n-1)]$, $(a_{n+2}, b_{n+2}) = (A_{n+2}^m, B_{n+2}^m)(n+m+2)(n+m+1)/[\omega a^2(2n+5)(2n+3)]$, α_0, β_0, a_{n_0}, b_{n_0} are the components of the forcing function, and d_1-d_{15} are the interaction coefficients, which are presented in explict form in Appendix 1.

In the adiabatic approximation, system (3) has two integrals of motion

$$\frac{d}{d\tau}\left[\frac{a_n^2 + b_n^2}{2} + \frac{15m\left[1 - \frac{12}{n(n+1)}\right]}{2d_9}\frac{(a_{n+2}^2 + b_{n+2}^2)}{2} + \frac{15m\left[1 - \frac{12}{n(n+1)}\right]}{2d_{12}}\frac{(a_{n-2}^2 + b_{n-2}^2)}{2} + \frac{4\alpha^2}{3n(n+1)N_n^m} + \frac{24\beta^2}{7n(n+1)N_n^m}\right] = 0, \quad (4)$$

$$\frac{d}{d\tau}\left[\frac{a_n^2 + b_n^2}{2} + \frac{d\left[1 - \frac{12}{n(n+1)}\right]}{d_9\left[1 - \frac{12}{(n+2)(n+3)}\right]}\frac{(a_{n+2}^2 + b_{n+2}^2)}{2} + \frac{d_5\left[1 - \frac{12}{n(n+1)}\right]}{d_{12}\left[1 - \frac{12}{(n-2)(n-1)}\right]}\frac{(a_{n-2}^2 + b_{n-2}^2)}{2} - \frac{a_n C}{n(n+1)} + \frac{8\alpha(\alpha-2)}{3n^2(n+1)^2 N_n^m} + \frac{288\beta^2}{7n^2(n+1)^2 N_n^m}\right] = 0 \left(N_n^m = \int_0^\pi (P_n^m)^2 \sin\theta\, d\theta\right) \quad (5)$$

one of which expresses the law of conservation of energy and the other the law of conservation of enstrophy.

In the general case of quasilinear system (2) there exists only one integral of motion, consisting of a combination of the integrals expressing the laws of conservation of energy and enstrophy [12].

Although the system under consideration is also quasilinear, by virtue of the special choice of reference functions (we consider only spherical functions with a single azimuthal index m), it is a special, degenerate case of the Galerkin approximation of the nonlinear equation of potential vorticity and thus is a system of the hydrodynamic type, with two quadratic integrals of motion, including a positive-definite quadratic integral, that of the energy.*

*When constructing the low-order model we began from approximate system (2) rather than from Eqs. (1) because in the general case of a description of orography in terms of spherical functions with different azimuthal index m, the structure of the system of equations in the low-order model remains quasilinear, so that the regular procedure can be used to find its steady-state solutions. Direct application of the Galerkin method to Eq. (1) would give rise to nonlinear terms consisting of products of components with different m in the equations describing the evolution of the nonzonal component of the flow. This would greatly complicate the procedure for finding steady-state solutions of the model.

It is evident from Eq. (5) that the larger the wave number n, i.e., the smaller the characteristic size of the topographic nonuniformities, the greater their role would be in the exchange of angular momentum between the atmosphere and the earth via interaction of Rossby waves with orography. Equation (5) also indicates that as the difference $n - m$ decreases, i.e., as the meridional scale of the orographic function increases, the exchange of angular momentum becomes more efficient.

Blocking is by definition a stationary or quasistationary process. Thus, studying the stationary solutions of the model bears directly on the theory of blocking. We seek steady-state solutions of Eq. (3) by the graphic method. Setting the right sides of Eqs. (3) equal to zero, we note that the last six equations are linear in the nonzonal components. Solving this linear system of equations, we find $a_{n-2}, b_{n-2}, a_n, b_n, a_{n+2}, b_{n+2}$ as functions of α and β. Then, treating α as an independent variable and using a numerical method to find for each value of α the corresponding value of β from the second equation of system (3), we construct the function $f(\alpha) = \alpha + d_3 C b_n(\alpha, \beta(\alpha))/\varepsilon$. The intersection of the plot of this function with the line $f = \alpha_0$ gives the value of α representing steady-state solutions of the model. These values of α are then used to find the values of the remaining components of the steady-state solutions.

Figure 1 shows a plot of $f(\alpha)$ for four different orographic functions, described respectively by spherical modes $C_4{}^3P_4{}^3 \sin 3\varphi$, $C_5{}^2P_5{}^2 \sin 2\varphi$, $C_6{}^3P_6{}^3 \sin 3\varphi$, $C_7{}^2P_7{}^2 \sin 2\varphi$. For each of the modes we present curves for three values of the Ekman relaxation coefficient ε, i.e., 0.01, 0.02 and 0.06, representing relaxation times τ_ε of 16, 8 and 2.7 days, and three values of the mean height of the mountains (in units of H_0),

$$h = \frac{\left(\iint (C_n^m P_n^m \sin m\varphi)^2 \, d\sigma\right)^{1/2}}{l_{\text{avg}} \sqrt{4\pi a^2}} = \frac{C\omega \sqrt{N_n^m}}{2l_{\text{avg}}}$$

i.e., 0.05, 0.1, and 0.15. It will be seen from the figure that the smaller the value of $n - m$ (i.e., the coarser the meridional structure of the orographic nonuniformities), the greater the change in $f(\alpha)$ as h and ε are varied. The function $f(\alpha)$ has between 2 and 4 maxima for the modes under consideration. When one of the parameters ε, h and α_0 changes while the others are held constant, successive bifurcations occur in which the number of steady-state solutions of Eq. (3) changes. For example, for the mode $\xi_6{}^3$ at $\varepsilon = 0.02$ and $h = 0.01$, as α_0 is varied from 0.08 to 0.18 the system has successively 1, 3, 5, 7, 5, 3 and 1 steady-state solutions (at the points $\alpha_0 = 0.09$, 0.125, 0.147, 0.157, 0.16, and 0.165, where the system has multiple roots, there exist 2, 4, 6, 4 and 2 different steady-state solutions). Even regimes with the same number of steady-state solutions are qualitatively different. We call attention to the relationships between the parameters under which the first bifurcation occurs. We will expect that as ε increases, the value of h at which the first transition occurs will increase. The minimum value of α_{tot} representing the first bifurcation for modes $\xi_6{}^3$ and $\xi_7{}^2$ rises monotonically with increasing ε, whereas for modes $\xi_4{}^3$ and $\xi_5{}^2$ it has a minimum in the interval $\varepsilon = 0.01$–0.06. It will be seen from the plots that owing to the nonlinearity of the system, variation in h and ε causes changes not only in the values of the extrema of $f(\alpha)$, but also in their positions, and leads to the appearance of new extrema and the disappearance of old ones.

Investigation of steady-state solutions of the model leads to the question of their stability. If the point representing a steady-state solution on the plot of $f(\alpha)$ lies within the zone where $\partial f(\alpha)/\partial\alpha < 0$, it can be demonstrated that the solution is unstable. This is proved in Appendix 2. The condition $\partial f/\partial\alpha < 0$ is a sufficient condition for instability. Our analysis does not allow of any assertions regarding steady-state solutions lying in the region $\partial f/\partial\alpha > 0$.

To study the behavior of nonlinear system (3) in the vicinity of steady-state solutions, the equations of system (3) were integrated with respect to time by the Runge-Kutta method. Figure 2 shows the results of integration of a system in which $\xi = C_7{}^2P_7{}^2 \sin 2\varphi$, $\alpha_0 = 0{,}19$; $\beta_0 = 0$, $a_{n_0} = 0$, $b_{n_0} = 0$, $\varepsilon = 0{,}01$; $h = C_7{}^2\sqrt{N_7{}^2}\omega/2l_{\text{avg}} = 0{,}149$. The steady-state solutions that were studied for stability and near which the initial values for integration of the system were chosen are numbered 1, 2 and 3 in Fig. 1d.

Figure 2 illustrates the temporal evolution of the component α of system 3. Curve a describes the behavior of mode α when perturbed solution 1 was chosen as an initial condition (Fig. 1d). The integration was performed over a period of 120 days. During this time, the components of the system made 3 or 4 fluctuations and reached the steady-state solution with respect to which they were perturbed. The period of the fluctuations was about 23 days. Both the period and the amplitudes of the fluctuations of the different modes were dependent on the magnitude and type of the initial perturbation. If the perturbation was not excessively large, the period changed little. Curve b represents steady-state solution 2, which is unstable according to our criteria. The system components fluctuate with a period of about 12–14 days and tend asymptotically to the values representing steady-state solution 1. With a second initial condition (with the perturbed value of α assumed to be greater than steady-state solution 2), the system passes into a state representing steady-state solution 3. Finally, line c repre-

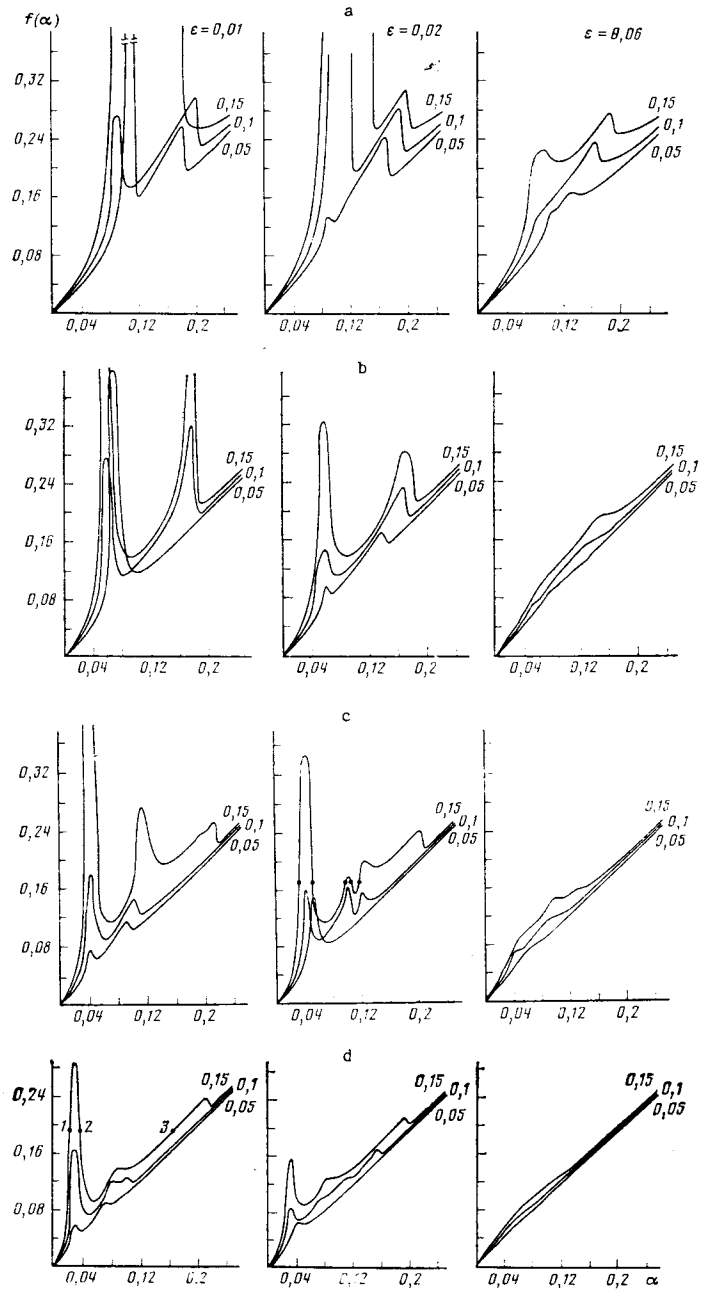

Fig. 1. Dependents of function $f(\alpha)$ on ε and h for orographic function described by modes ξ_4^3 (a), ξ_5^2 (b), ξ_6^3 (c) and ξ_7^2 (d).

sents the change in mode α of system (3) when the initial values were slightly different from those for steady-state solution 3; this solution, like solution 1, is stable.

Thus, numerical integration confirms that solution 2 is unstable, while solutions 1 and 3 prove to be stable. Note that a similar stability situation of the steady-state solutions was found by Charney et al. [3] and Källen [10], who calcuculated the eigenvalues of a matrix constructed from the coefficients of a system of linear equations dervied by linearization of a system analo-

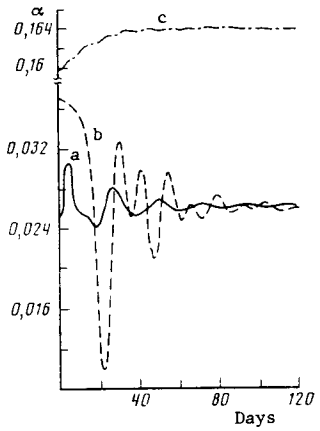

Fig. 2. Temporal evolution of component α obtained by integrating system (1), using as initial values (see Fig. 1d) slightly perturbed steady-state solution 1 (a), steady-state solution 2 (b) and steady-state solution 3 (c).

gous to (3) with respect to the steady-state solutions under consideration. The superresonant solutions also prove to be unstable and the subresonant solutions prove to be stable or very weakly unstable.

Stream function fields were constructed from the values of the components representing steady-state solutions. The flow patterns for the two cases in which the orographic function ξ was described by modes $C_6^3P_6^3\sin 3\varphi$ and $C_7^2P_7^2\sin 2\varphi$, are shown in Figs. 3 and 4, which also show the field of the orographic function for each case (Figs. 3f and 4d). It will be seen that for small values of the circulation index α, the flow pattern has the form typical of split blocking (Figs. 3a, b and 4a). An anticyclone is located in high latitudes and a cyclone in low latitudes, and a solitary cyclone occurs northwest of the pair. The pair is 15-20° east of the extreme values of the orographic function. The flow patterns shown in Figs. 3c, d, e and 4c represent a zonal type of atmospheric circulation and consist of an intense meandering zonal flow with a cyclone occurring downstream from the extremum of the orographic function. A comparison of Figs. 3 and 4 indicates that the latitude at which the center of the blocking pair occurs is strongly dependent on the meridional structure of the orographic function. Thus, to obtain a correct latitude distribution of the blocking pair with a low-order model, in our choice of an orographic function we must take account of the modes that give the most realistic meridional structure of the relief.

In conclusion, we emphasize again that the eight-component model used here is a simple self-consistent barotropic model describing the interaction of Rossby waves with a zonal flow different from solid rotation in the presence of orography. Within the limits of our expansion procedure, it takes account of all possible interactions between modes, making it possible to reconstruct the transitions of energy and entropy to both smaller-scale and larger-scale wave modes, which is particularly important when the mode generated by flow of a zonal mode over the terrain relief becomes barotropically unstable, thus allowing a more realistic description of the flow pattern in blocking structures that happen to be cases of resonance.

The author is grateful to M. V. Kurganskiy for useful discussions and support.

APPENDIX 1

$$d_1 = m\left(1-\frac{2}{n(n+1)}\right),\ d_2 =$$

$$= \frac{3}{2}m\left(1-\frac{12}{n(n+1)}\right)\left(1-5\frac{2n(n+1)-2m^2-1}{(2n+3)(2n+1)}\right),$$

$$d_3 = \frac{3}{8}mN_n^m,\ d_4 = \frac{7}{32}mN_n^m\left(1-5\frac{2n(n+1)-2m^2-1}{(2n+3)(2n-1)}\right),$$

$$d_5 = \frac{15}{2}m\frac{(n-2)(n-1)}{n(n+1)}\left(1-\frac{12}{(n-2)(n-1)}\right),\ d_6 =$$

$$= \frac{15}{2}m\frac{(n+2)(n+3)}{n(n+1)}\left(1-\frac{12}{(n+2)(n+3)}\right),$$

$$d_7 = m\left(1-\frac{2}{(n+2)(n+3)}\right),$$

$$d_8 = \frac{3}{2}m\left(1-\frac{12}{(n+3)(n+2)}\right)\left(1-5\frac{2(n+2)(n+3)-2m^2-1}{(2n+3)(2n+7)}\right),$$

$$d_9 = \frac{15}{2}m\frac{(n-m+1)(n-m+2)(n+m+1)(n+m+2)n(n+1)}{(2n+1)(2n+3)^2(2n+5)(n+2)(n+3)}\times$$

$$\left(1-\frac{12}{n(n+1)}\right),\qquad d_{10} = m\left(1-\frac{2}{(n-2)(n-1)}\right),$$

$$d_{11} = \frac{3}{2}m\left(1-\frac{12}{(n-2)(n-1)}\right)\times$$

$$\times\left(1-5\frac{2(n-2)(n-1)-2m^2-1}{(2n-5)(2n-1)}\right),$$

$$d_{12} = \frac{15}{2}m\frac{(n+m-1)(n+m)(n-m-1)(n-m)n(n+1)}{(2n-1)^2(2n+1)(2n-3)(n-2)(n-1)}\times$$

$$\left(1-\frac{12}{n(n+1)}\right),\ d_{13} = \frac{3m}{2n(n+1)}\left(1-5\frac{2n(n+1)-2m^2-1}{(2n+3)(2n-1)}\right),$$

$$d_{14} = \frac{15}{2}m\frac{(n-m+1)(n-m+2)}{(n+2)(n+3)(2n+1)}\times\frac{(n+m+1)(n+m+2)}{(2n+3)^2(2n+5)},$$

$$d_{15} = \frac{15}{2}m\frac{(n+m-1)(n+m)(n-m+1)(n-m)}{(n-2)(n-1)(2n+1)(2n-1)^2(2n-3)}.$$

APPENDIX 2

To prove that the steady-state solution satisfying the condition $\partial f(\alpha)/\partial\alpha|_{\alpha=\alpha_c}<0$ (where α_c is the value representing the steady-state solution)

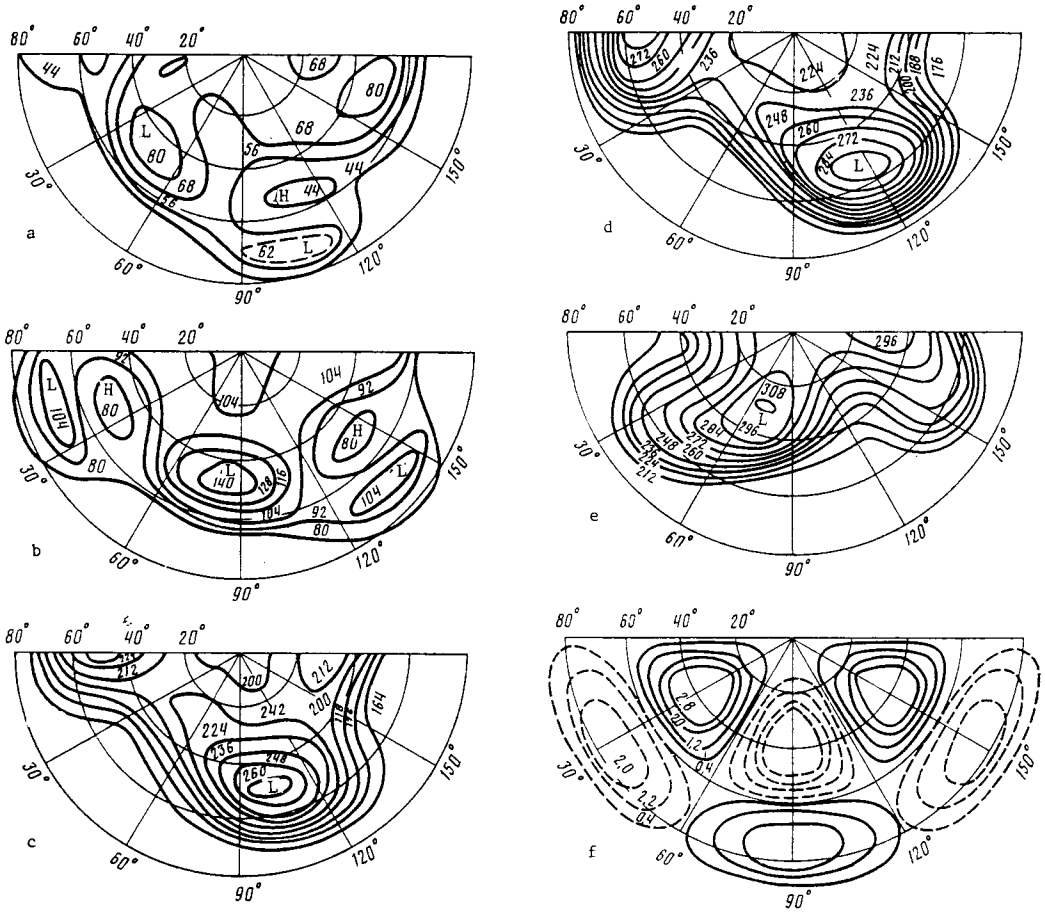

Fig. 3. Stream function fields (a-e) corresponding to steady-state solution (shown by points in Fig. 1c) and field of orographic function (e) when orography is described by mode ξ_6^3.

is unstable, it suffices to demonstrate that under this condition system (3) is unstable to perturbations of a particular type.

We consider the general case of an n-th order system

$$\frac{dx_1}{dt} = f_1(x_1 \dots x_n, x_{10}),$$
$$\frac{dx_2}{dt} = f_2(x_1 \dots x_n),$$
$$\dots\dots\dots\dots$$
$$\frac{dx_n}{dt} = f_n(x_1 \dots x_n).$$

Let functions f_i and their partial derivatives $\partial f_i/\partial x_i$ be continuous. Setting the time derivatives equal to zero and using the theorem of existence of implicit functions, we use the last $n-1$ equations to define $x_2, \dots x_n$ as functions of x_1, i.e., $x_2(x_1) \dots x_n(x_1)$. Substituting into the first equation, we find a steady-state solution as a function of the parameter x_{10}:

$$f_1(x_{1c}, x_2(x_{1c}) \dots x_n(x_{1c}), x_{10}) = \varphi(x_{1c}, x_{10}) = 0.$$

We now vary only x_1 from the steady-state value. The equations for the perturbations become

$$\frac{dx_1'}{dt} = \left.\frac{\partial \varphi}{\partial x_1}\right|_{x_1 = x_{1c}} x_1',$$
$$\frac{dx_2'}{dt} = \left(\frac{\partial f_2}{\partial x_1} + \frac{\partial f_2}{\partial x_2}\frac{dx_2}{dx_1} + \dots \frac{\partial f_2}{\partial x_n}\frac{dx_n}{dx_1}\right)\Bigg|_{x_1 = x_{1c}} x_1',$$
$$\dots\dots\dots\dots\dots\dots\dots\dots$$
$$\frac{dx_n'}{dt} = \left(\frac{\partial f_n}{\partial x_1} + \frac{\partial f_n}{\partial x_2}\frac{dx_2}{dx_1} + \dots \frac{\partial f_n}{\partial x_n}\frac{dx_n}{dx_1}\right)\Bigg|_{x_1 = x_{1c}} x_1'. \qquad (6)$$

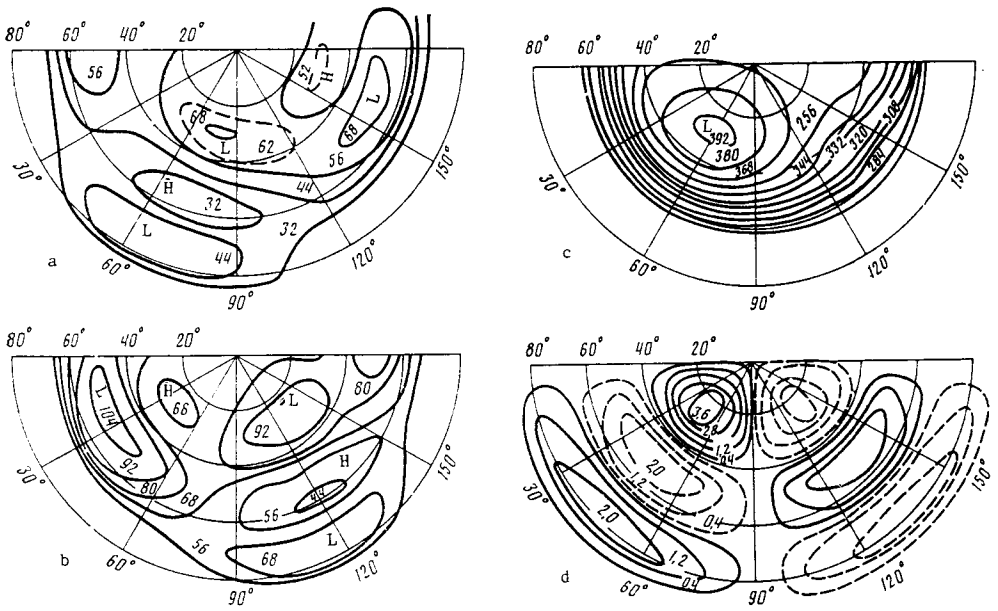

Fig. 4. Stream function fields (a-c) corresponding to steady-state solutions (shown by points in Fig. 1d) and field of orographic function (d) when orography is described by mode ξ_7^2.

We seek a solution of (6) in the form $(x_1' \dots x_n') = (\tilde{x}_1' \dots \tilde{x}_n')e^{\sigma t}$. The characteristic equation of the system is

$$\sigma^{n-1}\left(\sigma - \frac{\partial \varphi}{\partial x_1}\bigg|_{x_1=x_{1c}}\right) = 0.$$

Hence, if $\partial\varphi/\partial x_1|_{x_1=x_{1c}} > 0$, the steady-state solution is unstable. In the eight-component model under consideration, $\varphi(\alpha, \alpha_0) = \varepsilon\alpha_0 - \varepsilon f(\alpha)$, so that for $\partial f/\partial\alpha < 0$ the steady-state solution is unstable.

Received July 17, 1987;
revised November 20, 1987

REFERENCES

1. Obukhov, A. M., M. V. Kurganskiy, and M. S. Tatarskaya. Dynamic conditions of occurrence of droughts and other large-scale weather anomalies. Meteorologiya i gidrologiya, No. 10, 5-13, 1984.
2. Charney, I. G. and I. G. De Vore. Multiple flow equilibria in the atmosphere and blocking. J. Atmos. Sci., 36, No. 7, 1205-1216, 1979.
3. Charney, J. G., J. Shukla and K. C. Mo. Comparison of a barotropic blocking theory with observation. J. Atmos. Sci., 38, No. 4, 762-779, 1981.
4. Roads, J. O. Quasi-linear blocks forced by orography in a hemispheric, quasi-geostrophic barotropic model. Monthly Weather Rev., 109, No. 7, 1421-1437, 1981.
5. White, W. B. and N. E. Clark. On the development of blocking ridge activity over central North Pacific. J. Atmos. Sic., 32, No. 3, 489-502, 1975.
6. Egger, J. Dynamics of blocking highs. J. Atmos. Sci., 35, No. 10, 1788-1801, 1978.
7. McWilliams, J. C. An application of equivalent modons to atmospheric blocking. Dyn. Atmos. and Ocean., 5, No. 1, 43-66, 1980.
8. Gryanik, V. M. Singular geostrophic vortices on the β plane as a model of synoptic vortices. Okeanologiya, 26, No. 2, 174-179, 1986.
9. Galin, M. B. and S. Ye. Kirichkov. Effect of orography on nonzonal circulation of the

atmosphere and blocking structures. Iz. Akad. Nauk SSSR. Fiz. atmos. i okeana, 21, No. 7, 691-699, 1985.
10. Kallen, E. The nonlinear effects of orographic and momentum forcing in low-order barotropic model. J. Atmos. Sci., 38, No. 10, 2150-2163, 1981.
11. Paegle, J. N. The effect of topography on Rossby wave. J. Atmos. Sci., 36, No. 11, 2267-2271, 1979.
12. Pisnichenko, I. A. Allowance for orography in the problem of the movement of a barotropic atmosphere above a spherical earth. Izv. Akad. Nauk SSSR. Fiz. atmos. i. okeana, 22, No. 10, 1017-1025, 1986.